

# EPITAXIALLY INDUCED DEFECTS IN Sr- AND O-DOPED $\text{La}_2\text{CuO}_4$ THIN FILMS GROWN BY MBE: IMPLICATIONS FOR TRANSPORT PROPERTIES

J.-P. LOCQUET<sup>a\*</sup> AND E.J. WILLIAMS<sup>a,b</sup>

<sup>a</sup>IBM Research Division, Zurich Research Laboratory, 8803 Rüschlikon, Switzerland

<sup>b</sup>Département de Physique de la Matière Condensée, Université de Genève  
1211 Genève, Switzerland

In this paper, the critical role played by various types of defects and strain relaxation mechanisms in high- $T_c$  thin films is highlighted and illustrated with examples. The defects are essential for providing adequate diffusion channels for oxygen ingress during the cooling step in  $c$ -axis thin films. The operation of strain relaxation mechanisms necessitated by the lattice mismatch between film and substrate can impose a compressive or tensile biaxial pressure, which either increases or reduces the critical temperature.

PACS numbers: 61.72.Nn, 74.62.Fj, 81.15.Hi, 74.72.Dn

## 1. Introduction

Superconducting cuprate thin films are usually grown at *high temperatures on lattice-mismatched substrates*. These two experimental constraints however have huge implications for the quality of thin films. Thin-film growth is mostly a low oxygen pressure process, which implies — using the established phase diagrams — a serious oxygen deficiency at the high temperatures used (700–850°C). For instance, for the growth of  $\text{YBa}_2\text{Cu}_3\text{O}_7$  ('123') under these conditions, the oxygen content of the cuprate is close to 6.0 instead of the required content of 7.0 [1]. On cooling the film under oxidizing conditions after growth, oxygenation takes place; this correlates with a volume change [2] as well as with a tetragonal–orthorhombic phase transition [3]. While only the compounds containing chains, such as  $\text{YBa}_2\text{Cu}_3\text{O}_7$ ,  $\text{Y}_{1-x}\text{Pr}_x\text{Ba}_2\text{Cu}_3\text{O}_7$  and  $\text{LaBa}_2\text{Cu}_3\text{O}_7$ , require a very large uptake of oxygen (approx. from 6.0 to 7.0) during cooling [4], a similar process is necessary for other compounds, such as the  $\text{La}_{2-x}\text{Sr}_x\text{CuO}_4$  [5] or  $\text{La}_2\text{CuO}_{4+\delta}$  [6–13] cuprates, although their uptake of oxygen is much smaller ( $x/2$  and  $\delta$ , respectively). It is difficult to give an absolute estimate of the precise oxygen content of thin films. For this, Raman scattering [14] and oxygen desorption [15] have been proposed.

\*Corresponding author.

These methods allow a global oxygen content determination, which correlates only to a first order with the critical temperature. On a microscopic scale, the oxygen-oxygen repulsion often gives rise to a local oxygen ordering and hence to the presence of distinct superconducting phases having different  $T_c$ 's [16, 17].

It is clear that oxygenation during cooling is crucial for superconductivity. However, to optimize an oxidation treatment, the values of the oxygen-diffusion coefficients and their anisotropy must be taken as determining factors. Indeed, in the La-Sr-Cu-O system, *c*-axis thin films with sufficient structural quality can be grown rendering a post-growth oxidation nearly impossible. The first goal of this paper is to show that *additional defects*, such as planar faults and/or precipitates, both of which can serve as oxygen diffusion channels, *must be incorporated* in *c*-axis thin films to ensure adequate oxygenation for superconductivity.

The second important experimental constraint concerns the film growth on a lattice-mismatched substrate. The lattice misfit is generally accommodated by the introduction of misfit dislocations once a critical thickness ( $h_c$ ) which is determined by the lattice mismatch, nucleation mechanisms and the elastic properties of the material has been exceeded. However, for most high- $T_c$  thin films, the substrate surface imperfection, the formation of intermediary layers and the presence of secondary phase precipitates (Y-O [18], Cu-O [19] either on the surface or as inclusions), grain-, twin- and anti-phase boundaries, interstitials, and vacancies (in particular, oxygen) can relieve part of the lattice misfit. Only in the microstructurally best films, i.e. those without a large proportion of the above defects, is the strain relaxed by the appearance of a misfit dislocation network. This difference in microstructural quality easily explains the large spread in  $h_c$  (from 4 to 20 nm) observed for '123' thin films deposited on SrTiO<sub>3</sub> (STO) [20]. Furthermore, there have been few "direct" observations of the misfit dislocation network using transmission electron microscopy. For '214' thin films on (001) STO, the first such "direct" observation was reported some time ago [21].

While  $h_c$  is the thickness for which the first dislocations appears, the thickness for which the total strain is relieved,  $h_t$ , is much larger. For intermediate thicknesses only a part of the strain is relaxed, which allows the induction of a significant variable tensile or compressive lattice distortion, i.e. a "biaxial pressure" (plane strain) state similar to the "uniaxial" pressure experiments with the exception that cause and effect are reversed. Our next goal will be to show that the growth of thin *c*-axis La<sub>2-x</sub>Sr<sub>x</sub>CuO<sub>4</sub> films on substrates with a varying epitaxial strain allows the "biaxial pressure" dependence of the critical temperature to be studied, which for instance leads to a lowering of  $T_c$  by *ca.* 50% for thin films grown on (001) SrTiO<sub>3</sub>. On the other hand, a well-chosen compressive strain can lead to thin films whose  $T_c$  values exceed those of bulk compounds significantly.

An additional complication in this field of research is that these two experimental constraints, i.e. oxygen inclusion and epitaxial strain, are strongly correlated. Indeed, the lattice misfit at the growth temperature is determined by the difference in lattice parameters between a slightly oxygen-deficient perovskite (STO) and the "strongly" oxygen-deficient cuprate. Upon cooling, both lattices become smaller according to their respective thermal expansion coefficients. In ad-

dition, as more oxygen is inserted into the film lattice, the film lattice parameter can change significantly. These two effects can induce an additional tensile or compressive strain component.

Alternatively, the amount of oxygen incorporated upon cooling can also be a function of the already "compressive" or "tensile" state that decreases or increases the effective volume available for oxygen occupation.

## 2. Experimental

The oxygen- and strontium-doped '214' thin films were grown in a custom-designed molecular beam epitaxy (MBE) system equipped with two electron beam guns, four effusion cells, a reflection high energy electron diffraction (RHEED) system and an efficient atomic oxygen source derived from the Oxford Applied Research source. The efficiency of the original Oxford Applied Research RF source compares very favorably with other plasma sources, as discussed in [22]. The deposition method used is neither a codeposition method nor a layer-by-layer deposition but consists of a block-wise deposition of the various elements that is aimed at forming the desired compound only during the deposition of the final block with a minimum of intermediary phases [23, 24]. For the undoped '214' compound grown on STO, the probable interfacial stacking sequence is Sr-O — Ti-O — La-O — Cu-O — La-O (a similar stacking sequence was derived from high resolution electron micrography (HREM) images obtained on  $\text{La}_2\text{SrCu}_2\text{O}_8$  films deposited on  $\text{SrTiO}_3$  [25]); this would indicate an "ideal" sequential layer-by-layer deposition procedure of 1 monolayer of La-O, followed by 1 monolayer of Cu-O and finally another monolayer of La-O before the entire sequence is repeated. Such a process sequence is not optimal because once the Cu-O monolayer has been deposited, '214' will start to form, leaving about half the deposited Cu-O as precipitates. Hence, the preferred block-by-block sequence consists of the deposition of 2 monolayers of La-O followed by 1 monolayer of Cu-O.

The properties of such films deposited on (001) (STO, in tension) or (001)  $\text{SrLaAlO}_4$  (SLAO, in compression), whether doped with strontium or oxygen, have already been studied. The strontium-doped films were used to study the doping dependence of the penetration depth [26] and coherence length [27], while the oxygen-doped films were used to demonstrate the electrochemical oxidation of *c*-axis films [7, 28] as well as local electrochemical lithography [8].

## 3. Results and discussion

The '214' films used were between 50 and 200 nm thick. The X-ray diffraction patterns of these films typically display single-phase *c*-axis epitaxy with finite-size oscillations at low angles and around the *c*-axis reflections [29] (50 nm thick films). Accordingly, the atomic force microscope images indicate a film surface that is smooth and has large terraces and steps of 0.66 nm, i.e. half the structural unit cell. The overall roughness is of the order of 1 to 2 unit cells [29], with the occasional appearance of either Cu-O or La-O precipitates, depending on the precise flux composition.

## 3.1. Oxidation

As discussed in the introduction, the thin films must undergo a post-growth oxygen annealing step (which usually takes place in the growth chamber, *in situ*) during cooling. Under these conditions, the oxygen uptake is essentially governed by the diffusion coefficient. Layered compounds such as the cuprates exhibit a strong anisotropy in the diffusion coefficients.

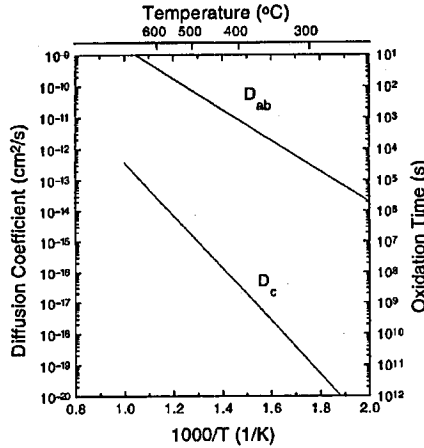


Fig. 1. In-plane and out-of-plane diffusion coefficients as a function of the inverse temperature. The right axis indicates the time required to oxidize a 100 nm thick film as estimated from the diffusion coefficient on the left axis.

In Fig. 1 the diffusion coefficients along the *ab*-planes ( $D_{ab}$ ) and parallel to the *c*-axis ( $D_c$ ) derived from measurements on '123' single crystals [30] are shown as a function of the inverse temperature. On the right-hand side, the time ( $t$ ) necessary to oxidize a 100 nm thick ( $d_f$ ) sample was estimated using the diffusion relation  $d_f = \sqrt{(D_c \times t)}$ . From this figure, it is clear that the oxidation plateau at 400–450°C during the cooling of "perfect" *c*-axis '123' thin films requires an extremely long annealing time of about  $10^8$ – $10^9$  s. However, as soon as sufficient defects with a component along the *c*-axis exist in the thin film (they operate as fast oxygen diffusion channels), the oxidation behavior is dominated by the in-plane diffusion coefficient. Indeed, at those temperatures  $D_{ab}$  is four to five decades larger than  $D_c$ , and the required annealing times become reasonable and in agreement with the experimental findings of *ca.*  $10^3$ – $10^4$  s.

The figure clearly illustrates the necessity of defects (oxygen channels) for the oxidation of *c*-axis '123' thin films. As the reported diffusion coefficients for the strontium-doped '214' compounds are similar to those mentioned above [31], defects will also be required. Typical '123' thin films have a sufficient number of microstructural defects so that the annealing process does not pose a problem; however, the structural quality of some '214' films grown more recently was such

that the oxidation process (whether during cooling under atomic oxygen or during an electrochemical treatment) turned out to be impossible on a reasonable time scale. Hence, one must address the crucial question as to which microstructural features provide the means for adequate oxygen diffusion.

The unit cell of '214' is peculiar in that, when viewed in the (114) plane, the presence of potential oxygen interstitial sites becomes apparent [32]. Probably for precisely this reason, bulk specimens of this compound can be oxidized at room temperature under an electrochemical potential in a 1 mole KOH solution [6]. Hence this compound represents a model system in which oxygen diffusion can be readily studied. We have recently shown that this simple electrochemical process is also applicable for *c*-axis thin films [7, 8, 28]. However, we have also speculated that a particular type of microstructural feature is a prerequisite for the proper functioning of the electrochemical oxidation: the presence of planar faults [28].



Fig. 2. Bright-field image of a cross-sectional specimen showing that faults (labeled 'F') extend through the thickness of this material, from [21].

The bright-field image (Fig. 2) of a cross-sectional specimen obtained using a transmission electron microscope (TEM) reveals these planar faults lying on the four {101} tetragonal or equivalent {111} orthorhombic planes; they occur across the entire thin film [21] with an average separation of  $50 \pm 10$  nm. Their occurrence and density, however, vary from one film to the next. In addition these faults penetrate the full thickness of the film as can easily be seen in the figure. Lattice imaging indicates that they also contain a shear component similar to that reported earlier [33]. The electrochemical oxidation process and, in particular, the plateau measured during the first  $I(V)$  curve of a fresh sample [28] were correlated to the presence of a significant density of planar faults in thin films grown on STO.

This study was further extended to thin films deposited on other substrates with varying tensile or compressive misfits;  $\text{NdGaO}_3$ ,  $\text{LaAlO}_3$  and SLAO. The '214' thin films grown on these substrates can all be oxidized electrochemically [34]. A systematic TEM analysis reveals that all these films indeed have a varying density of planar faults [35]. On the other hand, a number of thin films recently grown on both STO and SLAO could not be oxidized electrochemically, and their  $I(V)$

curves did not show an oxidation plateau (see for instance [28]). Accordingly, their microstructure shows either the absence of planar faults [28] or the presence of a different type of fault; a detailed report comparing the microstructure of "oxidizable" and "nonoxidizable" films is currently in preparation [36]. The planar faults provide just one type of oxygen diffusion channels. Other channels that have been identified in these films are related to the appearance of Cu-rich and La-rich precipitates.

It is currently not clear which experimental parameters determine the appearance of the planar faults. As indicated above, neither the sign nor the magnitude of the lattice mismatch seem to be a major controlling factor. The actual composition of the thin film also appears to be only a minor factor, as the planar faults appear in both Cu-O and La-O rich films as well as in films with and without Sr doping. The other experimental factors which could have an influence are: (i) the substrate miscut, (ii) the cooling procedure, (iii) the atomic oxygen pressure during growth and (iv) the details of the initial crystal nucleation process. Nevertheless, the above analysis indicates that in *c*-axis thin films a certain type of defect with a significant density is crucial in order to obtain the oxygen content necessary for the occurrence of superconductivity. Further work must focus on identifying the mechanisms involved in generating these defects as well as on providing a systematic tuning of their size and density in order to optimize the oxidation behavior. Although the examples discussed here are related to the '214' compound, the same general conclusions apply for other oxide films.

Having discussed the macroscopic "average" values of the *c*-axis and in-plane diffusion coefficients and having identified the microstructural channels providing "easy" oxygen ingress, let us now address the issues related to the diffusion on the nanoscale. Optimum superconducting properties can only be obtained in thin films if the desired oxygen content has been attained during cooling and if that oxygen is homogeneously distributed. In particular the transition width ( $\Delta T_c$ ), defined for instance as the temperature difference between 90% and 10% of the resistance, seems to be a good indication of the homogeneity of the superconductor. Typical transition widths in cuprate thin films are of the order of 1–2 K, a factor of ten to one hundred times larger than those obtainable for classical low-temperature superconductors.

The oxygen vacancy sites which must be filled in the strontium-doped '214' compound can be in the apical position (O2) as well as in the CuO<sub>2</sub> plane (O1). For the optimally doped compound ( $x = 0.15$ ), about 0.075 oxygen atoms per unit cell must be incorporated in the lattice upon cooling, i.e. one atom in every 12–13 unit cells. Hence, the occurrence of oxygen vacancies in two neighboring unit cells is probably very rare. On the other hand, for the same compound about 0.15 La<sup>3+</sup> atoms have been replaced by 0.15 Sr<sup>2+</sup> atoms per unit cell, i.e. one substitution every 6–7 unit cells. As every unit cell is surrounded by eight neighboring cells (four nearest-neighbors and four next-nearest-neighbors), considering only a two-dimensional plane, this means that every strontium atom has at least one other strontium atom among its neighboring unit cells. Hence it is plausible that an oxygen site close to or in between two such strontium-containing unit cells remains vacant during the growth. The "random" distribution of strontium atoms

in the unit cell will plausibly lead to a "random" distribution of such vacancies. During cooling, oxygen must diffuse from the planar faults into these vacant sites at a speed given by the corresponding diffusion coefficient. Close to the "ideal" full occupation, the chemical potential becomes small and other interactions, such as the oxygen-oxygen repulsion, become dominant, thereby providing higher energy barriers for oxygen diffusion and probably preventing homogeneous oxidation.

### 3.2. Lattice mismatch

#### 3.2.1. Structural properties: tensile mismatch

In this section, the physical properties related to the difference in the lattice parameters of film and substrate are discussed. For '214' thin films (50 nm thick) on (001) STO, we have shown that the in-plane lattice parameter at the growth temperature and the  $c$ -axis lattice parameter at room temperature are larger and smaller, respectively, than the values derived for bulk samples [26].

The evolution of the  $c$ -axis lattice parameter with the strontium content for '214' films on STO is shown in Fig. 3. These data are in very good agreement with those recently reported for codeposited (MBE) [37], sputtered [38, 39] and laser-ablated '214' thin films [40, 41]. Although there is an experimental error ( $\pm 0.01 \text{ \AA}$ ) in the determination of the  $c$ -axis lattice parameter for the thin films, a comparison between the data for films and bulk materials indicates an average difference of  $0.03\text{--}0.06 \text{ \AA}$ , which increases with the strontium content in the range  $0.07 \leq x \leq 0.24$ . Such an increase in compression of the  $c$ -axis must be coupled via Poisson's ratio to an increased expansion of the in-plane lattice parameters. Experimental facts support this hypothesis: (i) the *in situ* measurement during growth of the in-plane lattice parameters obtained from RHEED data [26] (shown below in Fig. 4) and (ii) the average separation between the misfit dislocations which reflects the difference in lattice parameters: despite a decrease in the in-plane lattice parameters with strontium doping for bulk compounds, the dislocation spacing observed for the thin films does not vary significantly [42], suggesting a more constant  $a$ -axis value as reported in Fig. 5. Hence, it seems that with a higher strontium content also a higher degree of tensile strain is incorporated.

Before proceeding, we must estimate at which point the misfit dislocation network is formed. From the RHEED data shown in Fig. 4 [26], it seems that the lattice mismatch starts to be relieved at a thickness of 5 to 7 unit cells (i.e.  $h_c$  between 65 and 90  $\text{\AA}$ ). The evolution of the [100] and [110] lattice parameters is presented as a function of the number of deposited unit-cells. The extrapolated bulk '214' values (3.826  $\text{\AA}$  and 2.703  $\text{\AA}$ , respectively) are indicated by the short lines on the corresponding axis. For the first 5–7 unit cells, the in-plane lattice parameter is very close to that of the substrate, but for larger thicknesses, as the creation of misfit dislocations sets in, a decrease in the lattice parameters is observed. However, even for the largest thickness in this experiment, the thin film values are still significantly larger than the bulk lattice parameters, suggesting that the strain is not yet completely relieved. Nonetheless, these results confirm that most of the misfit is relaxed during growth.

In summary, the data suggest that the films on STO have an in-plane tensile strain that leads to a measurable decrease in the  $c$ -axis lattice parameter of about

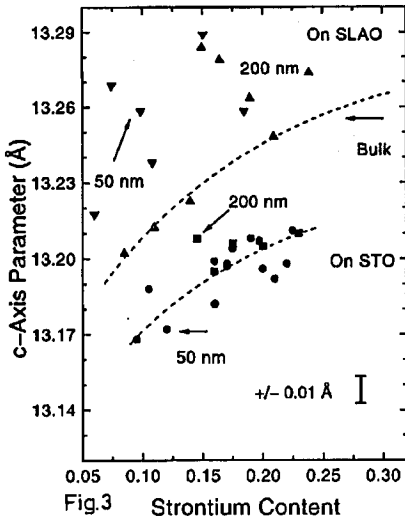


Fig.3

Strontium Content

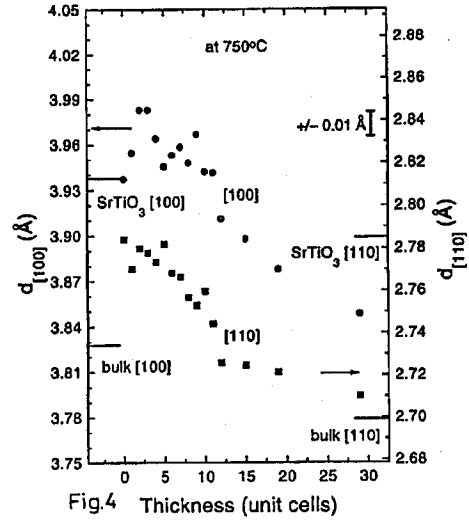


Fig.4

Thickness (unit cells)

Fig. 3. Evolution of the *c*-axis lattice parameter with Sr content for bulk samples (dashed lines), 50 nm (●) and 200 nm (■) thick films on STO and 50 nm (full ∇) and 200 nm (full Δ) thick films on SLAO.

Fig. 4. Evolution of the in-plane  $d_{100}$  (●) and  $d_{110}$  (■) lattice parameters as a function of thickness for an undoped '214' film.

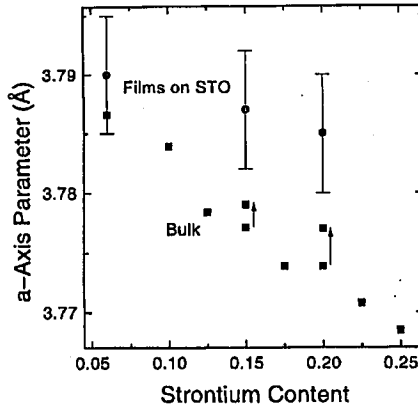


Fig. 5. Evolution of the in-plane lattice parameter with Sr content for bulk samples (■, Ref. [47]) and 50 nm thick (●) films on STO estimated from the misfit dislocation network. The change of the in-plane lattice parameter after annealing in vacuum is indicated by the arrows for the bulk samples with  $x = 0.15$  and  $0.20$ .

0.03–0.06 Å. Under *hydrostatic* pressure at room temperature, the compressibility of the optimally doped '214' compound along each crystallographic direction  $u$ ,  $\kappa_u = \partial \ln(u) / \partial P$  is nearly equal to  $2.2 \times 10^{-3} \text{ GPa}^{-1}$  [43]. Hence under hydrostatic conditions, a decrease in the lattice parameters of the magnitude observed for

the  $c$ -parameter would require 1–2 GPa. For the case of thin films, however, the in-plane lattice parameters are modified by the epitaxy, and the  $c$ -parameter adjusts accordingly with the film surface acting as a free surface. This situation is thus comparable to that of *uniaxial* compression along the  $c$ -axis. If only the  $c$ -axis is to be compressed (by 0.03–0.06 Å), a lower pressure than for the hydrostatic case will be necessary. Hence the hydrostatic case provides an upper limit estimate of the required uniaxial pressure necessary to produce such lattice parameter changes in the '214' compound.

Unfortunately, the literature provides no values for the change in the lattice parameters under uniaxial pressure, but a simple estimate of the pressure ( $P$ ) required under these conditions can be made when Young's modulus ( $Y = 191$  GPa), Poisson's ratio ( $\nu = 0.315$ ) for the '214' compound [44] and the relations  $\Delta c/c = P/Y$ ,  $\Delta a/a = -\nu P/Y$  are known. Applying these relations leads to a required uniaxial pressure between 0.45 and 0.9 GPa, which will increase the in-plane lattice parameter by 0.01–0.02 Å, in agreement with the experimental data derived from measurements of the dislocation spacings (Fig. 5).

During cooling, the difference in thermal expansion coefficients between film and substrate can induce an additional strain. However, this strain is unlikely to relax via the nucleation of misfit dislocation because not enough thermal energy is available for efficient nucleation or propagation once the film has reached a temperature at which the thermal misfit becomes significant. Nevertheless, the thermal expansion coefficients of STO and '214' suggest an in-plane compression of the thin film upon cooling which partially compensates for the in-plane expansion due to the lattice mismatch.

### 3.2.2. Structural properties: compressive mismatch

The use of a substrate imposing a compressive epitaxial strain (SLAO) for the preparation of superconducting '214' thin films was reported a few years ago [40]. In Fig. 3, we add some of our recent data points (50 nm thick '214') for films deposited on SLAO<sup>†</sup> to those of 200 nm thick films deposited on the same substrate reported in the literature [37]. Despite significant scatter in the two data sets, the  $c$ -axis lattice parameters of these films are generally equal to or larger than those of the bulk compounds. As a film becomes thicker, more compressive strain is relieved and the  $c$ -axis lattice parameter approaches that of the bulk compound. The largest  $c$ -axis lattice parameter obtained (for 50 nm optimally doped films) was 13.29 Å, which is 0.06 Å larger than the corresponding bulk value and about 0.11 Å larger than the average value for films deposited on STO. This impressive increase in the  $c$ -axis lattice parameter for the films under a small in-plane compressive misfit ( $\approx 1\%$ ) must be compared to a similar decrease in the  $c$ -axis under a relatively large tensile misfit ( $\approx 3\%$ ).

---

<sup>†</sup> There is a significant uncertainty in the actual determination of the strontium and oxygen content of these films, and the value of the resistivity was used to estimate the effective strontium content [45].

### 3.2.3. Structural properties: oxygen incorporation

A further complication involves the "small" oxygen uptake as the film cools under oxidizing conditions. The amount of oxygen incorporated (*in the apical O sites*) during cooling for an optimally doped '214' thin film corresponds to about 0.075 (4.00–3.925). Unfortunately, little data is available in the literature regarding the evolution of the lattice parameters of strontium-doped '214' with the oxygen content. However, examples include the slight increase [46] of the  $c/a$  ratios of strontium-doped single crystals and bulk samples during oxygen annealing as well as the reduction of the  $c$ -lattice parameter and increase in the in-plane lattice parameters [47] of  $x = 0.15$  and 0.2 bulk samples when reduced under a reduced oxygen atmosphere (see arrows in Fig. 5). Upon annealing nearly optimally strontium-doped '214' thin films in vacuum at moderate temperatures ( $\approx 300^\circ\text{C}$ ), the oxygen ( $\approx x/2$ ) taken up during cooling can be removed. This leads to a decrease in the  $c$ -axis by about 0.026 Å, as shown in Fig. 6. This behavior is similar to the evolution of the ( $c$ -axis and in-plane) lattice parameters of the "interstitially" oxygen-doped '214' compound [48, 49], also indicated in Fig. 6. In both cases the oxygen uptake leads to a significant increase in the  $c$ -axis lattice parameter and a decrease in the in-plane lattice parameter, despite the fact that the additional oxygen occupies different lattice sites. Furthermore, the changes observed upon oxygen incorporation are of the same magnitude as those induced by strontium doping.

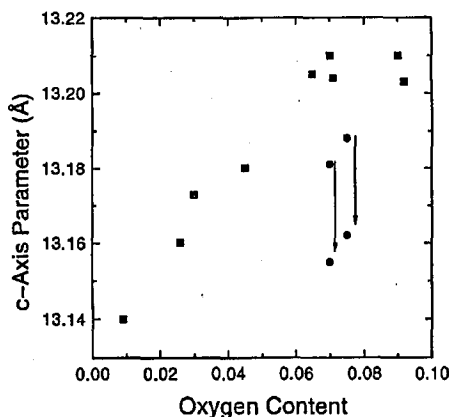


Fig. 6. Evolution of the  $c$ -axis lattice parameter with oxygen content for bulk samples (■). The change in the  $c$ -axis lattice parameter for two 50 nm Sr-doped films on STO ([Sr] = [2 O]) (●) before and after an *ex situ* reduction experiment is shown by the arrows.

From this analysis, two important conclusions can be drawn. First, for strontium-rich films, an oxygen deficiency during growth will give rise to a *significantly larger in-plane lattice parameter* than that expected for bulk oxidized material. The critical thickness ( $h_c$ ) and the density of misfit dislocations as a function of thickness will be determined by this expanded in-plane lattice pa-

parameter (which is clearly even further expanded thermally). The reported change upon oxidizing the reduced Sr-doped compound [47] is of the order of 0.003 to 0.005 Å, which is about the half of that reported for oxygen-doped '21.1' bulk samples [48, 49]. In the last case, the decrease in the in-plane lattice parameter for an interstitial oxygen content increasing between 0.0 and 0.06 — which is "charge equivalent" to the amount of oxygen uptake for a film with a strontium content between 0.0 and 0.12 — is about 0.013 Å on 3.80 Å (averaged over the *a* and *b*-axes). Secondly, upon oxygen incorporation during cooling, the in-plane lattice parameter will tend to reduce, thus increasing (for (001) STO substrates, but reducing for "compressive" substrates) the tensile strain remaining in the film.

Can these two effects also explain the apparent increase in the retained tensile strain with increasing strontium content and the asymmetric misfit dependence of the *c*-axis lattice parameter of '214' thin films? As the strontium content increases, the in-plane thermal expansion coefficient also seems to increase slightly (unfortunately no high-temperature data exist; the preceding statement has been derived from measurements between 50 K and 295 K [50]). Hence, with increasing strontium content the in-plane compression upon cooling due to the thermal mismatch becomes larger, leaving a larger tensile strain in these films, in agreement with the experimental data. In addition, the oxygen deficiency in the film during growth also increases as the strontium content increases, leading to larger in-plane film lattice parameters from which the lattice mismatch and the dislocation network are defined. Indeed, the network is a reflection of the lattice misfit at the growth conditions (determined by the lattice parameters, the thermal expansivities and the oxygen deficiency), and is "frozen in" during cooling. Both arguments (thermal misfit and oxygen deficiency) point in the same direction, thus explaining the increased tensile strain with strontium doping.

As the films are cooled, sufficient oxygen might be expected to be incorporated to restore the lattice parameters to their bulk values. For optimally doped films, the increase in the *c*-axis lattice parameter due to oxygen incorporation is of the order of 0.03 Å. This change in lattice parameter must be combined with that already induced by the lattice mismatch. This should be incorporated in an explanation of the asymmetric misfit dependence of the *c*-axis lattice parameter, i.e. the strong increase in the *c*-axis lattice parameter for a small (1%) compressive mismatch compared to a similar decrease for a much larger (3%) tensile mismatch. However, another reason for this asymmetry may be the relative bond lengths, energies, positions and orientations within the unit cell, all of which may cause the somewhat different behaviors under tension and compression.

So far, we have assumed here that the lattice distortions imposed upon the film do not significantly modify the amount of oxygen taken up during cooling or the diffusion coefficients. However, this is not at all guaranteed. For instance, it is known that for bulk compounds the *c*-axis lattice parameter reaches a maximum at a strontium content of *ca.* 0.3 [47], owing to the fact that the vacant apical sites can no longer all be filled with oxygen. For thin films on STO, this maximum seems to be shifted to lower strontium contents, about 0.23 (Fig. 3), suggesting that under tensile strain these apical sites are even more difficult to fill.

This discussion has been mainly qualitative in order to illustrate the various effects; a clear experimental separation of them currently remains impossible. To disentangle these effects it requires a precise measurement of (i) the lattice parameters during growth, (ii) the thermal expansion coefficients of the substrate and the thin films, and (iii) the oxygen contents incorporated during growth and during cooling. In addition, for films on STO and on SLAO considerable scatter is present in the data, which suggest that both the oxygen content and the residual strain vary from one sample to the other. Nevertheless, it has become clear from the above discussion that particularly for thin films with an excellent microstructure in epitaxial contact with a substrate, the structural properties must differ considerably from those of the bulk compounds.

### 3.2.4. Transport properties

Finally, not only the structural properties are affected by a tensile or compressive residual strain, but also the transport properties in the normal and the superconducting state. The critical temperature ( $T_c$ ) versus  $x$  was measured both resistively and inductively, and is shown in Fig. 7 for both thin and thick films prepared on STO substrates under identical conditions.

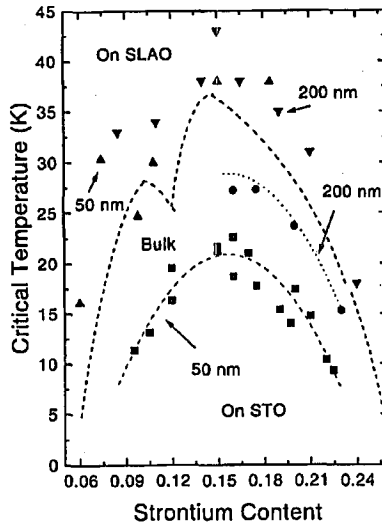


Fig. 7. The critical temperature as a function of Sr concentration for bulk samples (dashed curves) for thin (39, 50 and 65 nm: ■) and thick (200 nm: ●) films on STO and 50 nm (full  $\Delta$ ) and 200 nm (full  $\nabla$ , Ref. [38]) thick films on SLAO.

At optimal doping for the thickest films the maximum critical temperature observed is about 28 K; away from optimal doping, the critical temperature decreases. The observed maxima of 23 K and 28 K for thin and thick films, respectively, are in good agreement with those reported in the literature [37, 41]. The structural study presented above indicates the presence of significant tensile strain, i.e. a negative "biaxial" pressure of the order of 0.45–0.9 GPa, which can be com-

pared with the “uniaxial” pressure dependence of  $T_c$ . To our knowledge, only one direct experiment of the uniaxial pressure dependence of the critical temperature is available in the literature. Motoi et al. [51] studied this property on grain-aligned ‘214’ composites as a function of Sr doping, and found that  $T_c$  decreases at the rate of 3 to 9 K/GPa under pressure applied along the  $c$ -axis, depending on the doping level. Hence the strongly reduced critical temperature for thin films on STO can be explained by the estimated “biaxial” tension.

For thicker films more strain is relieved (although the extent differs from sample to sample, see Fig. 3), the critical temperature is indeed higher, but the general trend of  $T_c$  versus  $x$  is the same for both thicknesses (see Fig. 7). Indeed, it is well known that applying pressure to this high- $T_c$  cuprate changes the *absolute values* of the critical temperature but only weakly affects the *general trend* of the superconducting properties (for instance, the maximum of  $T_c(x)$  still occurs for  $x \simeq 0.16$ ).

In Fig. 7, some of our data points obtained from 50 nm thick ‘214’ films deposited on SLAO [45] are presented together with recent literature values for 200 nm thick films [37]. For the same thickness, the critical temperature of thin films deposited on SLAO is considerably higher than that of those deposited on STO and, in general, even higher than that of bulk compounds. The optimally doped 50 nm thin film has a  $T_c$  (zero resistance) of 38 K, close to the highest value reported for bulk compounds. However, the critical temperature, 43.7 K, of the 200 nm optimally doped films in the literature [37] is more than 5 K higher than the highest reported bulk value. This impressive result demonstrates that *the  $T_c$  in thin films can be increased significantly by a compressive in-plane strain*.

At first glance these latest results also contain a contradiction, i.e. thicker films should have relaxed more strain and hence should have a critical temperature closer to that of the bulk. Indeed some of the 200 nm thick films on SLAO have a  $c$ -axis lattice parameter close to that of bulk samples and smaller than that of 50 nm films. However, they still seem to have a higher critical temperature than the bulk samples and the 50 nm films. On the other hand, some of the 200 nm thin films grown on SLAO have a very large  $c$ -axis lattice parameter compared to the bulk values, particularly those films with the highest critical temperatures. These facts, together with the significant scatter in the data, point again to the above arguments, in that both the *additional compressive strain* (induced upon cooling owing to the thermal misfit and/or the oxygen uptake) and the *amount of oxygen incorporation* (induced upon cooling but determined by the density and nature of the faults in the film) can differ considerably from sample to sample.

Still, these results leave a number of questions unanswered. For instance, it is not clear why the increase in  $T_c$  is only 5 K for an increase in the  $c$ -axis of 0.06 Å, while a decrease of about 10 K is observed for a corresponding decrease in the  $c$ -axis. As there are no data for the crystal structure regarding its uniaxial pressure dependence, one can only speculate that the atomic displacements (Cu-O1 and Cu-O2 bond lengths) in the unit cell are not symmetrical when applying pressure. In addition, kinetic inductance measurements of our 50 nm thick films grown on SLAO systematically show a mixed phase behavior [45], partially confirmed by a structural gradation observed in X-ray diffraction for 500 nm thick films on

SLAO [37]. The origin of this mixed phase behavior is as yet unknown and subject to further study.

#### 4. Summary

As the structural quality of cuprate oxide thin films has improved significantly, the role played by defects as well as by strain relaxation mechanisms has become increasingly important. We have discussed their effects on the structure and the transport properties. First, the importance of *adequate oxygen diffusion channels*, necessary for oxygen ingress during cooling, was demonstrated. In the case of the '214' compound, the presence of planar faults in sufficient density was found to be suitable for the oxidation process. Secondly, the role of strain relaxation mechanisms was illustrated by comparing the structural and physical properties of '214' films under compressive and tensile strain. A *strong increase in the c-axis lattice parameter and in the critical temperature*, compared with bulk material, was reported.

#### Acknowledgments

We would like to thank the following colleagues, who have contributed over the years towards the achievements of these results: F. Arrouy, Y. Jaccard, A. Daridon, J. Perret, J. Fompeyrine, E. Mächler, C. Gerber, P. Bauer, R. Berger, C. Rossel, M. Despont, P. Martinoli, Ø. Fischer and H. Siegenthaler; also the group at Bordeaux, J.-C. Grenier, A. Wattiaux and C. Monroux for their guidance in the field of electrochemical oxidation. We acknowledge stimulating and encouraging discussions with K.A. Müller, J.G. Bednorz and P. Guéret. Support for this work from the Schweizerischer Nationalfonds zur Förderung des Wissenschaftlichen Forschung, Project NFP 30, is also gratefully acknowledged.

#### References

- [1] B.T. Ahn, T.M. Gür, R.A. Huggins, R. Beyers, E.M. Engler, *Mater. Res. Soc. Symp. Proc.* **99**, 171 (1988); B.T. Ahn, T.M. Gür, R.A. Huggins, R. Beyers, E.M. Engler, P.M. Grant, S.S.P. Parkin, G. Lim, M.L. Ramirez, K.P. Roche, J.E. Vasquez, V.Y. Lee, R.D. Jacowitz, *Physica C* **153-155**, 590 (1988); R. Bormann, J. Nölting, *Appl. Phys. Lett.* **54**, 2148 (1989).
- [2] H. Strauven, J.-P. Locquet, O.B. Verbeke, Y. Bruynseraede, *Solid State Commun.* **65**, 293 (1988).
- [3] I.K. Schuller, D.G. Hinks, M.A. Beno, D.W. Capone II, L. Soderholm, J.-P. Locquet, Y. Bruynseraede, C.U. Segre, K. Zhang, *Solid State Commun.* **63**, 385 (1987).
- [4] J.-P. Locquet, J. Vanacken, B. Wuyts, Y. Bruynseraede, K. Zhang, I.K. Schuller, *Europhys. Lett.* **7**, 469 (1988).
- [5] R.B. Van Dover, R.J. Cava, B. Batlogg, E.A. Rietman, *Phys. Rev. B* **35**, 5337 (1987).
- [6] A. Wattiaux, J.C. Park, J.-C. Grenier, M. Pouchard, *C.R. Acad. Sci. II* **310**, 1047 (1990).
- [7] J.-P. Locquet, C. Gerber, A. Cretton, Y. Jaccard, E.J. Williams, E. Mächler, *Appl. Phys. A* **57**, 211 (1993).

- [8] J.-P. Locquet, F. Arrouy, E. Mächler, M. Despont, P. Bauer, E.J. Williams, *Appl. Phys. Lett.* **68**, 1999 (1996).
- [9] M. Ronay, M.A. Frisch, T.R. McGuire, *Phys. Rev. B* **45**, 355 (1992).
- [10] H. Zhang, H. Sato, G.L. Liedl, *Physica C* **234**, 185 (1994).
- [11] R. Decca, D. Serafini, F. de la Cruz, J. Abriata, *Phys. Rev. B* **48**, 4014 (1993).
- [12] V.I. Simonov, L.A. Muradyan, R.A. Tamazyan, V.V. Osiko, V.M. Tatarintsev, K. Gamayumov, *Physica C* **169**, 123 (1990).
- [13] K. Yoshimura, Y. Nishizawa, Y. Ueda, K. Kosuge, *J. Phys. Soc. Jpn.* **59**, 3073 (1990).
- [14] K.Y. Yang, H. Homma, R. Lee, R. Bhadra, M. Grimsditch, S.D. Bader, J.-P. Locquet, Y. Bruynseraede, I.K. Schuller, *Appl. Phys. Lett.* **53**, 808 (1988).
- [15] B. Wuyts, J. Vanacken, J.-P. Locquet, C. Van Haesendonck, I.K. Schuller, Y. Bruynseraede, in: *Proc. NATO ASI Series, Physics and Material Science of High Temperature Superconductors, Bad Winheim, Germany, Aug. 13-26, 1989*, Ed. R. Kosowsky, Kluwer, Dordrecht 1990, p. 307.
- [16] J.-P. Locquet, J. Vanacken, B. Wuyts, Y. Bruynseraede, I.K. Schuller, *Europhys. Lett.* **10**, 365 (1989).
- [17] E.J. Williams, W.M. Stobbs, *Inst. Phys. Conf. Ser.* **119**, Sec. 7, 311 (1991); *idem*, *Philos Mag. A* **68**, 1 (1993).
- [18] A. Catana, R.F. Broom, J.G. Bednorz, J. Mannhart, D.G. Schlom, *Appl. Phys. Lett.* **60**, 1016 (1992).
- [19] J.-P. Locquet, Y. Jaccard, C. Gerber, E. Mächler, *Appl. Phys. Lett.* **63**, 1426 (1993).
- [20] J.-P. Contour, A. Défossez, D. Ravelosona, A. Abert, P. Ziemann, *Z. Phys. B* **100**, 185 (1996).
- [21] E.J. Williams, J.-P. Locquet, E. Mächler, Y. Jaccard, A. Cretton, R.F. Broom, C. Gerber, T. Schneider, P. Martinoli, Ø. Fischer, *Inst. Phys. Conf. Ser.* **138**, Sec. 7, 329 (1993).
- [22] J.-P. Locquet, E. Mächler, *J. Vac. Sci. Technol. A* **10**, 3100 (1992).
- [23] J.-P. Locquet, A. Catana, E. Mächler, C. Gerber, J.G. Bednorz, *Appl. Phys. Lett.* **64**, 372 (1994).
- [24] J.-P. Locquet, E. Mächler, *MRS Bulletin XIX*, 39 (1994).
- [25] K. Verbist, G. Van Tendeloo, private communication.
- [26] J.-P. Locquet, Y. Jaccard, A. Cretton, E.J. Williams, F. Arrouy, E. Mächler, T. Schneider, Ø. Fischer, P. Martinoli, to appear in *Phys. Rev. B*.
- [27] Y. Jaccard, T. Schneider, J.-P. Locquet, E.J. Williams, P. Martinoli, Ø. Fischer, *Europhys. Lett.* **34**, 281 (1996).
- [28] F. Arrouy, J.-P. Locquet, E.J. Williams, E. Mächler, R. Berger, C. Gerber, C. Monroux, J.-C. Grenier, A. Wattiaux, to appear in *Phys. Rev. B*.
- [29] Y. Jaccard, A. Cretton, E.J. Williams, J.-P. Locquet, E. Mächler, C. Gerber, T. Schneider, Ø. Fischer, P. Martinoli, in: *Proc. SPIE Conf. on Oxide Superconductor Physics and Nanoengineering, January 26-28, 1994, Los Angeles*, Ed. D. Pavuna, Vol. 2158, SPIE, Bellingham (WA) 1994, p. 200; *idem*, *Physica C* **235-240**, 1811 (1994).
- [30] S.J. Rothman, J.L. Routbort, U. Welp, J.E. Baker, *Phys. Rev. B* **44**, 2326 (1991).
- [31] E.J. Opila, H.L. Tuller, B.J. Wuensch, *J. Am. Ceram. Soc.* **76**, 236 (1993).

- [32] C. Monroux, Ph.D. Thesis, University de Bordeaux, Bordeaux 1996.
- [33] J. Galy, *Acta Crystallogr. B* **48**, 777 (1992).
- [34] A. Daridon, H. Siegenthaler, F. Arrouy, E.J. Williams, E. Mächler, J.-P. Locquet, in: *Proc. E-MRS Spring Meeting 1996 on High Temperature Superconductor Thin Films, June 4-7, 1996, Strasbourg, France*, to appear in *J. Alloys Compounds*.
- [35] E.J. Williams, A. Daridon, F. Arrouy, J. Perret, Y. Jaccard, J.-P. Locquet, E. Mächler, H. Siegenthaler, P. Martinoli, Ø. Fischer, in: *Proc. E-MRS Spring Meeting 1996 on High Temperature Superconductor Thin Films, June 4-7, 1996, Strasbourg, France*, to appear in *J. Alloys Compounds*.
- [36] E.J. Williams, A. Daridon, F. Arrouy, J. Fompeyrine, H. Siegenthaler, E. Mächler, P. Martinoli, Ø. Fischer, to appear in *Proc. MRS Full Meeting 1996, Symposium P, Electrochemical Synthesis and Modification of Materials, 2-6 December 1996, Boston (USA)*.
- [37] H. Sato, M. Naito, *Physica C* **274**, 221 (1997).
- [38] H. Takagi, B. Batlogg, H.L. Kao, J. Kwo, R.J. Cava, J.J. Krajewski, W.F. Peck, Jr., *Phys. Rev. Lett.* **69**, 2975 (1992); H.L. Kao, J. Kwo, R.M. Fleming, M. Hong, J.P. Mannearts, *Appl. Phys. Lett.* **59**, 2748 (1991).
- [39] M. Suzuki, *Phys. Rev. B* **39**, 2312 (1989); M. Suzuki, M. Hikita, *ibid.* **44**, 249 (1991).
- [40] M.Z. Cieplak, M. Berkowski, S. Guha, E. Cheng, A.S. Vagelos, D.J. Rabinowitz, B. Wu, I.E. Trofimov, P. Lindenfeld, *Appl. Phys. Lett.* **65**, 3383 (1994); I.E. Trofimov, L.A. Johnson, K.V. Ramanujacharu, S. Guha, M.G. Harrison, M. Greenblatt, M.Z. Cieplak, P. Lindenfeld, *Appl. Phys. Lett.* **65**, 2481 (1994).
- [41] G. Rietveld, M. Glastra, D. van der Marel, *Physica C* **241**, 257 (1995).
- [42] E.J. Williams, J.-P. Locquet, A. Cretton, Y. Jaccard, Ø. Fischer, P. Martinoli, T. Schneider, in: *Proc. 13th Int. Congress on Electron Microscopy (ICEM 13)*, Eds. B. Jouffrey, C. Colliex, J.-P. Chevalier, F. Glas, P.W. Hawkes, Vol. 2B, Les Editions de Physique, Paris 1994, p. 987; E.J. Williams, A. Cretton, Y. Jaccard, J.-P. Locquet, E. Mächler, P. Martinoli, Ø. Fischer, in: *Proc. Microscopy & Microanalysis*, Eds. G.W. Bailey, M.H. Ellisman, R.A. Hennigar, N.J. Zaluzec, Jones & Begell Publishing, New York 1995, p. 382.
- [43] J.S. Schilling, S. Klotz, in: *Physical Properties of High Temperature Superconductors*, Ed. D.M. Ginsberg, Vol. 3, World Scientific, London 1992, p. 59.
- [44] J. Dominec, *Supercond. Sci. Technol.* **6**, 153 (1993).
- [45] J. Perret, Y. Jaccard, E.J. Williams, J.-P. Locquet, Ø. Fischer, P. Martinoli (in preparation).
- [46] P.J. Picone, H.P. Jenssen, D.R. Gabbe, *J. Crystal Growth* **91**, 463 (1988).
- [47] J.-M. Tarascon, L.H. Greene, W.R. McKinnon, G.W. Hull, T.H. Geballe, *Science* **235**, 1373 (1987).
- [48] J.-C. Grenier, F. Arrouy, J.-P. Locquet, C. Monroux, M. Pouchard, A. Villesuzanne, A. Wattiaux, in: *Phase Separation in Cuprate Superconductors*, Eds. E. Sigmund, K.A. Müller, Springer-Verlag, Berlin 1994, p. 236.
- [49] J.-C. Grenier, N. Lagueyte, A. Wattiaux, J.-P. Doumerc, P. Dordor, J. Etourneau, M. Pouchard, J.B. Goodenough, J.S. Zhou, *Physica C* **202**, 209 (1992).
- [50] M. Braden, P. Schweiss, G. Heger, W. Reichardt, Z. Fisk, K. Gamayunov, I. Tanaka, H. Kojima, *Physica C* **223**, 396 (1994).
- [51] Y. Motoi, K. Fujimoto, H. Uwe, T. Sakudo, *J. Phys. Soc. Jpn.* **60**, 384 (1991).